Characterization of a Porphyrin-Containing Dye-Sensitized Solar Cell

Jack Jasieniak,[‡,†] Martin Johnston,[‡] and Eric R. Waclawik*[,§]

Flinders University, School of Chemistry, Physics and Earth Sciences, Bedford Park, Adelaide, SA, Australia, and Queensland University of Technology, Inorganic Materials Research Program, School of Physical and Chemical Sciences, GPO Box 2434, Brisbane, QLD, Australia 4001

Received: May 5, 2004; In Final Form: June 8, 2004

The photovoltaic performance of several porphyrin-derivatized TiO_2 films in regenerative photoelectrochemical cells is reported and compared to that in cells sensitized with a Ru(2,2′-bipyridyl-4,4′-dicarboxylate)$_2$(NCS)$_2$ (N3) dye. The porphyrin sensitizers tetrakis(3′,5′-di-*tert*-butylphenyl)porphyrin, tetrakis(3′,5′-di-*tert*-butylphenyl)porphyrin zinc(II), and tetrakis(4'-carboxyphenyl)porphyrin were studied. Differences in efficiencies of the porphyrin light absorbers are ascribed to poor electronic coupling of the latter two sensitizers to the titania conduction band. Dark currents and $I-V$ curves were measured as a function of incident ligth intensity and I_3^-/I^- electrolyte concentrations for three different film preparations, with and without a coadsorber. Analysis of dark current results with use of a perviously proposed model suggests that the lower efficiencies yielded with P25 TiO_2 supports compared to semitransparent electrodes can be explained, in part, by the differneces in the measured back electron transfer. Photoaction spectra closely matched the prophyrin absorption spectra which we argue is more likely than for similar spectra reported previously in P25 films.

Introduction

Interest in the use of porphyrins as light-absorbing sensitizers in electrochemical photovoltaics has intensified over recent years, due in part to our better understanding of the role porphyrin molecules play in the natural photosynthetic process.[1,2] The photosynthetic components form into large antenna arrays in order to funnel energy into a reaction center of high enough redox potential for oxidation of water to occur. The chlorophyll and porphyrin-containing thylakoid membranes are also structured into grana lamellae within the chloroplast of the cell to enhance the active surface area and thus maximize light absorption.[2] While the assembly of similar highly complex heterogeneous systems into artificial energy conversion systems is still not technically feasible, several attempts have been made to use porphyrins as the active component in a variety of simpler man-made solar cells.[3−5] Rather than creating antennae, these devices employ a photoactive molecule that is bound to a semiconductor surface which can directly inject an electron into the device following light absorption.[6]

The incorporation of porphyrin molecules as the active component in solar cells has contributed a great deal to our understanding of the photovoltaic mechanism in these photoelectrochemical cells.[3] A notable study in this regard is the study by Bard and co-workers, who discovered that a liquid crystalline porphyrin sandwiched between two sheets of conductive tin oxide-coated glass displayed a significant photovoltaic effect under simulated solar irradiation conditions.[3] Their studies revealed that a photovoltaic effect can be produced in a heterojunction device in the absence of a built-in electric field (such as exists in a typical $p-n$ junction semiconductor solar cell).[4] The charge-transfer mechanism leading to this phenomenon was eventually agreed to be the process of interfacial exciton dissociation. Build-up of charge carriers either side of the interface between two phases, i.e., at the heterojunction, creates a concentration gradient of charged species, which provides the thermodynamic driving force for the flow of charge, and allows useful work to be performed by the system. In deference to the mechanism that is believed to drive these types of sandwich photovoltaic cells, they are sometimes called Excitonic Solar Cells, or XSCs.[4]

The most efficient type of XSC developed to date is the dye-sensitized solar cell (DSSC).[7] As demonstrated by O'Regan and Grätzel in 1991, with the right choice of sensitizing dye and redox couple electrolyte, DSSCs constructed from porous nanocrystalline titania can achieve excellent sunlight to electrical power conversion efficiencies of just over 10% under standard AM1.5 (the standard solar spectrum for temperate latitudes is Air Mass 1.5, or AM1.5, corresponding to the sun being at an elevation of 42°) light conditions.[7] Important requirements for highly efficient DSSC operation are the choice of sensitizing dye and redox electrolyte.[8] To date metal polypyridine complexes such as N3 and the black dye have proven to be by far the most effective sensitizing dyes in DSSCs.[8] There are several reasons for the effectiveness of this class of dye: their absorption spectra are well matched to the AM 1.5 solar spectrum, their incident photon-to-current efficiencies (ICPE) are practically quantitative over the visible region of the spectrum, they possess extraordinary electron injection rates, and back-electron transfer is slow.[8,9]

Besides polypyridyl complexes a variety of alternative sensitizers have been explored in dye-sensitized solar cells, in particular, the porphyrin and phthalocyanine classes of dye.[6,10,11] For instance, Grätzel and co-workers investigated the use of a variety of chlrophyll derivatives and related meso porphyrins: studying $I-V$ characteristics, DSSC performance, and the photosensitization mechanism of these species.[11] Although they could obtain good overall efficiencies, up to 2.6%, they noted that electron injection into the semiconductor oxidized the

‡ Flinders University.
† Current Address: University of Melbourne, Department of Chemistry, Melbourne, VIC, Australia.
§ Queensland University of Technology.

10.1021/jp048073i CCC: $27.50
Published on Web 07/22/2004

chlorophyll to a cation radical. Cation radicals are considered to be susceptible to side reactions and this was expected to drastically reduce the lifetime of an operational solar cell.[11] Of particular interest to the present study are studies of titania DSSCs sensitized with anionic porphyrins. One such study employing [tetrakis(4′-carboxyphenyl)porphyrinato]zinc(II) (or ZnTCPP) obtained the low ICPE of 40%. The electrolyte in this case consisted of a 0.1 M $NaClO_4$ solution containing 0.01 M hydroquinone.[5] More recent studies of tetrakis(4′-carboxyphenyl)porphyrin (TCPP)-sensitized DSSCs obtained similar overall energy conversion efficiencies; however, large discrepancies in overall IPCE were reported.[12−14]

Herein we describe our studies of porphyrin DSSCs in which we have studied the role of the porphyrin ground- and excited-state redox potentials and the linker group (to the titania electrode) and the effect of metalation of the porphyrin on IPCE, open circuit voltage (V_{oc}), short circuit currents (I_{sc}), and dark currents. The photoelectrochemical performances of three porphyrin dyes were investigated in this context, tetrakis(3′-5′-ditertbutylphenyl)porphyrin, TDTBPP, tetrakis(3′,5′-ditertbutylphenyl)porphyrin zinc(II), ZnTDTBPP, and TCPP. DSSC performance was compared to an N3-sensitized DSSC as a standard. In the course of the investigations it became clear that some inconsistencies in the IPCE photoaction spectra and V_{oc} values existed between previous studies of the same and similar porphyrin systems in DSSCs.[12−14] Interpretation of the previously published results in light of this new investigation has been made.

Experimental Section

To properly assess the performance of DSSCs sensitized with porphyrin dyes, semitransparent electrodes were required. To this end studies were performed with use of conductive glass coated with a 10 μm thick film of annealed (ca. 10-nm diameter) anatase titania nanoparticles. Results were compared throughout against electrodes produced from P25 (Degussa) titania colloid and with Ru(2,2′-bipyridyl-4,4′-dicarboxylate)$_2$(NCS)$_2$ (N3 dye) kindly donated by Sustainable Technologies International.

Synthesis of Porphyrin Dyes. All solvents used for organic synthesis were AR grade unless otherwise stated. 4-Carboxy benzaldehyde was purchased from Aldrich and used without purification and TCPP was prepared by using a method adapted from Datta-Gupta and Bardos.[15] 3,5-Ditertbutylbenzaldehyde was synthesized following the method of Newman and Lee[16] with TDTBPP and ZnTDTBPP prepared according to the method of Crossley.[17]

Electrode Preparation. Electrodes were prepared on NEC 15Ω fluorine-doped tin oxide (FTO) glass. Titania electrodes were prepared from a sol−gel, using a similar approach to that described by O'Regan and Grätzel.[18] Briefly, 2-propanol (20 mL) and titanium isopropoxide (125 mL) were placed into a 150 mL dropping funnel. This mixture was added dropwise over 10 min to deionized water (750 mL) under vigorous stirring. Hydrolysis occurred immediately and a white precipitate formed. After the alkoxide solution had been washed with water, nitric acid (5.3 mL, 69%) was added to act as a peptising agent. The solution was heated in a water bath at 80 °C for 8 h. During this time isopropoxide and some water evaporated, with the remaining solution (ca. 650 mL) obtaining an opaque white color. The resulting sol was stable with no precipitation evident over five months.

Approximately 150 mL of this TiO_2 solution was transferred into a hydrothermal bomb and placed into a 200 °C furnace for 16 h. Upon cooling, the solution was concentrated to ca. 170 g of TiO_2 per liter of solution with a rotary evaporator to produce a viscous solution. Prior to film production, 40 wt % of Carbowax 6000 was added to the sol with vigorous stirring for 1 h. The Carbowax acted both as a spreading agent and to enhance the final film porosity. This mixture was doctor bladed onto the support to create a 0.63 cm^2 active area. Room temperature drying for 1 h resulted in the film changing from opaque to completely colorless. Finally the electrodes were sintered in air at 400 °C, creating a clear, crack-free, high-surface area support consisting of interconnected 10−15 nm TiO_2 particles as confirmed by SEM, XRD, and Raman analysis (see Figure 1). For comparison, crack-free P25-based electrodes were prepared according to previously described procedures.[13,19]

The sensitizing dyes were applied to the electrodes by treating the electrodes for 24 h in a 0.1 mM TCPP dye solution containing 2 mM deoxycholic acid coadsorbent. An ethanolic solution of 1 mM N3 was used to prepare the N3 electrodes. TDTBPP and ZnTDTBPP were dissolved in cyclohexane to give a total concentration of 10 mM and required 36 h of exposure to the electrode. Prior to exposure to the dye solutions, all films were heated to 100 °C for a minimum of 1 h to remove surface-bound water molecules. An FTO counter electrode containing a catalytic coating of platinum was used to complete the DSSCs.

Equipment and Instrumentation. All UV−vis spectra were measured with a Varian Cary 50 Probe spectrophotometer. IPCE measurements were performed by passing the output of a 150-W xenon arc lamp through a Czerny-Turner spectrometer (5-cm^{-1} resolution) and a Schott KG4 filter to simulate the solar spectrum. Incident power was measured with use of a BPW21 photodiode and measurements recorded with an ADC-200 Pico data-logger.

Dark currents were measured on a Princeton Applied Research Potentiostat Model 273A. For both the dark and illuminated results, the system electrode was the working electrode (i.e., blank FTO, titania film, etc.) and the platinized electrode was made both the counter and reference electrode. Two setups were used for illuminated measurements. For low-power measurements a custom-built IR filter was used, while for high-power measurements a 10 nm path length water filter was used. $I-V$ characteristics were obtained on a Wenking LB75L Laboratory model potentiostat with incident power rating measured on a Molectron PowerMax 5000 detector. Final results were average results of at least two different cells.

Redox-Couple Selection and Properties. The active surface area of the DSSC was 0.63 cm^2 and the electrolyte mixture was 0.5 M LiI and 0.05 M I_2 in propylene carbonate. The redox couple plays a pivotal role in the regenerative nature of the DSSC, its main purpose, to contribute to charge separation by removing the hole of oxidized dye molecules from the exciton formation region.[8] The oxidized redox species then diffuses through the electrolyte to the counter electrode. Diffusion limitations are not normally noticeable in low light conditions.[20] However, when electron turnover is high (i.e. large photocurrents), diffusion rates become important and severe limitations in the performance can result. This is discussed in relation to our observations below.

Results

The films constructed were initially examined by using scanning electron microscopy and the results are shown in Figure 1. It is evident that clear titania films consisted of a network of large agglomerates of particles approximately 60 nm in diameter at the surface. Upon closer inspection these agglomerates were seen to be composed of a number of sintered

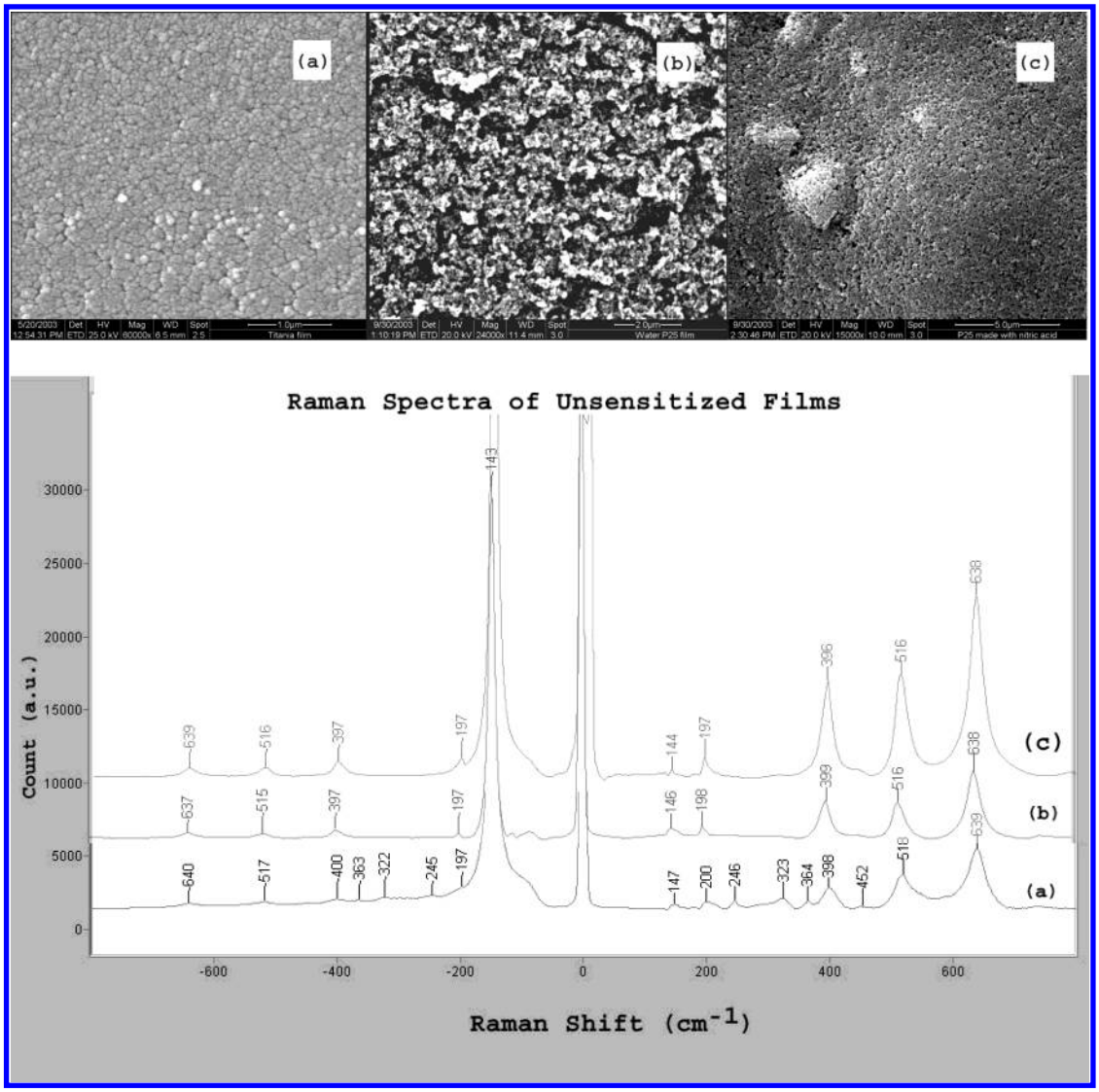

Figure 1. (a) SEM image of the clear titania film. Particles forming the surface layer are approximately 60 nm in diameter. Upon closer inspection the agglomerates were seen to be composed of a number of sintered nanoparticles (ca. 15 nm in diameter). (b) SEM image of a P25 titania film prepared by using the water-based method.[13] (c) SEM image of a P25 titania film prepared by using the nitric acid-based method.[19] (d) Raman spectra of the various titania films: factor group analysis showed the anatase structure to be the predominant titania phase present. Peaks located at (±)145, 200, 398, 519, and 638 cm^{-1} were previously assigned to the E_g, E_g, B_{1g}, A_{1g}/B_{1g}, and E_g modes of anatase.[35] No intense rutile peaks were observed (which was confirmed by XRD). Weak peaks at (±)246, 322, and 364 cm^{-1} are assigned to 2nd-order scattering.[34]

nanoparticles (ca. 15-nm diameter). The P25 films produced by using a water-based synthetic procedure possessed a far more open and porous structure;[13] this highly porous structure was not observed when we prepared P25 films using a nitric acid treatment.[19] The Raman spectra of the various films were recorded in an effort to ascertain the dominant phase of material present (Figure 1d). Analysis of the Raman spectra revealed anatase to be the predominant titania phase in all cases.

The clear titania films exhibited an absorption onset at 380−390 nm that corresponds directly to the characteristic 3.3 eV band-gap for this material.[21] Between 900 and 400 nm the rise in the apparent absorption profile in Figure 2 is gradual until 350 nm whereupon it rapidly begins to rise. In contrast to such a clearly defined absorption, P25 films strongly scattered the incident light and the absorption onset could not be clearly identified. This light scattering associated with 25 nm diameter TiO_2 particle films obscured the TiO_2 absorption spectrum below 500 nm and has prevented other authors from estimating quantum efficiency from IPCE results (action spectra) for TCPP at precisely the point where dye absorption is expected to be highest (the porphyrin Soret band maximum).[13,14] The use of near-transparent titania films in this work enabled both UV−vis and IPCE measurements to be performed up to the onset of the TiO_2 conduction band edge as can be seen in Figures 3 and 4, respectively.

The porphyrin-based DSSCs were compared to a cell sensitized with the N3 dye. As can be seen in Figure 3, absorption of N3 onto the titania surface caused a strong red shift owing to a change in the polarity of its environment, which modifies the $t_{2g} \rightarrow \pi^*$ MLCT transitions. The red shift is of the order of 20 nm, causing the maximum absorbance of this dye to coincide with the maximum power of the solar spectrum (i.e. ∼550 nm). In comparison, porphyrins exhibit two distinct regions in their UV−vis absorption spectra. The most intense absorption band, commonly referred to as the Soret band, exists in the 400−430-nm region. The Soret band is clearly the most intense peak observed in Figure 3 for all the porphyrin-based sensitizers investigated in this work. The free base porphyrins TCPP and TDTBPP possess four absorption bands in the 500−650-nm region. These peaks are collectively termed the Q-bands.

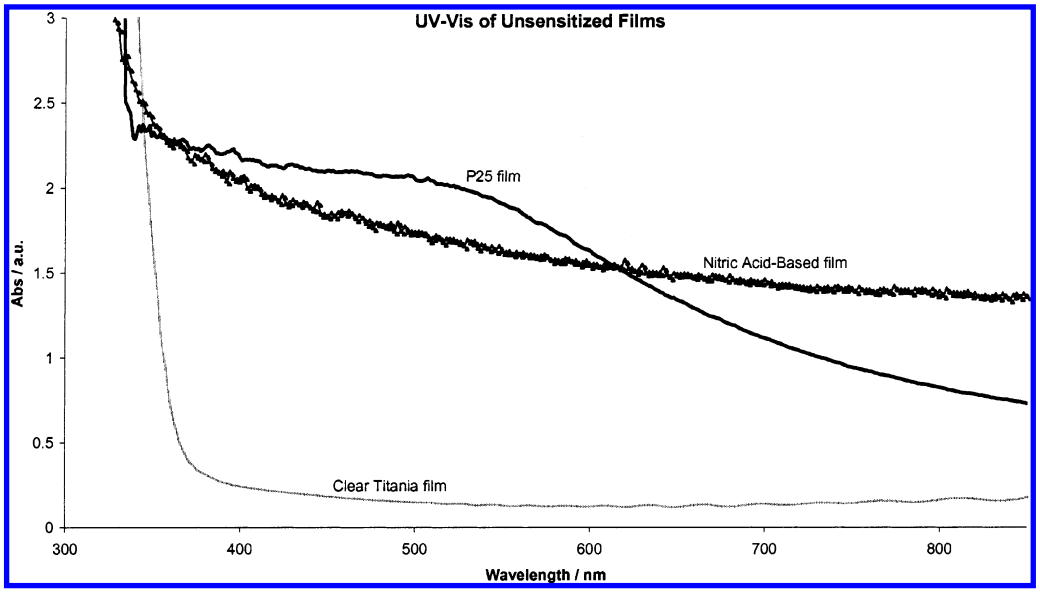

Figure 2. Comparison of UV−visible absorption spectra of transparent TiO_2 and P25 films prepared by water[13] and nitric acid-based[19] methods, respectively.

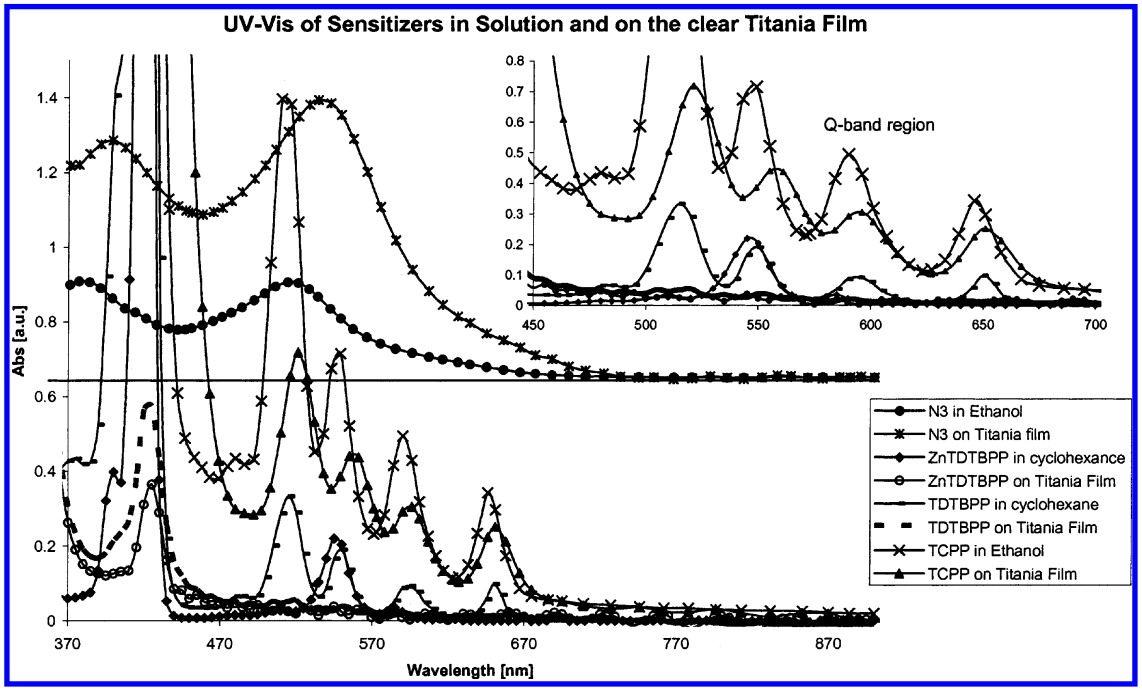

Figure 3. The UV−visible absorption spectra of the various dyes used in this work. Baselines of some spectra have been shifted to better visualize spectral features of the different dyes.

Q-bands of metalated porphyrins such as ZnTDTBPP exhibit two absorptions in this region, a consequence of a lowering of the porphyrin symmetry due to metalation.[22] From inspection of the spectra in Figure 3 it is evident that adsorption by TCPP is considerably larger than that for TDTBPP and ZnTDTBPP with these titania films. This is a direct consequence of the ability of TCPP to chemically bind to titania nanoparticles through their carboxylic acid moieties. The 5−10-nm red shift in the TCPP Q-band absorption peak upon binding to the substrate has previously been interpreted as being due to the change in polarity the dye molecule experiences upon chemisorption.[22] Of interest here is the shoulder appearing near 480 nm in the ethanol solution at high TCPP concentrations. Porphyrins such as TCPP tend to aggregate readily in solution, which causes a spectral blue shift.[23] Upon chemisorption of TCPP to the titania electrode this peak was not observed, which we interpret as an indication that surface aggregation was minimal. Monolayer coverage on the titania substrate was expected with little coplanar aggregation of TCPP.[13]

Incident Photon-to-Current Conversion Efficiencies. IPCE measurements were performed to compare the efficiency of each sensitizer over the sunlight spectral region. The IPCE can be related to the observed photocurrent density (J in μA/cm^2), the incident wavelength of light (λ in nm), and the incident power density (P_{inc} in μW/cm^2) through the following equation:

$$\mathrm{IPCE}(\lambda) = \frac{1243.5 \times I\,(\mu\mathrm{A/cm^2})}{\lambda\,(\mathrm{nm}) \times P_{\mathrm{inc}}\,(\mu\mathrm{W/cm^2})} \qquad (1)$$

The incident power density in these measurements was quite low (maximum of ∼140 μW/cm^2 at 550 nm) and power

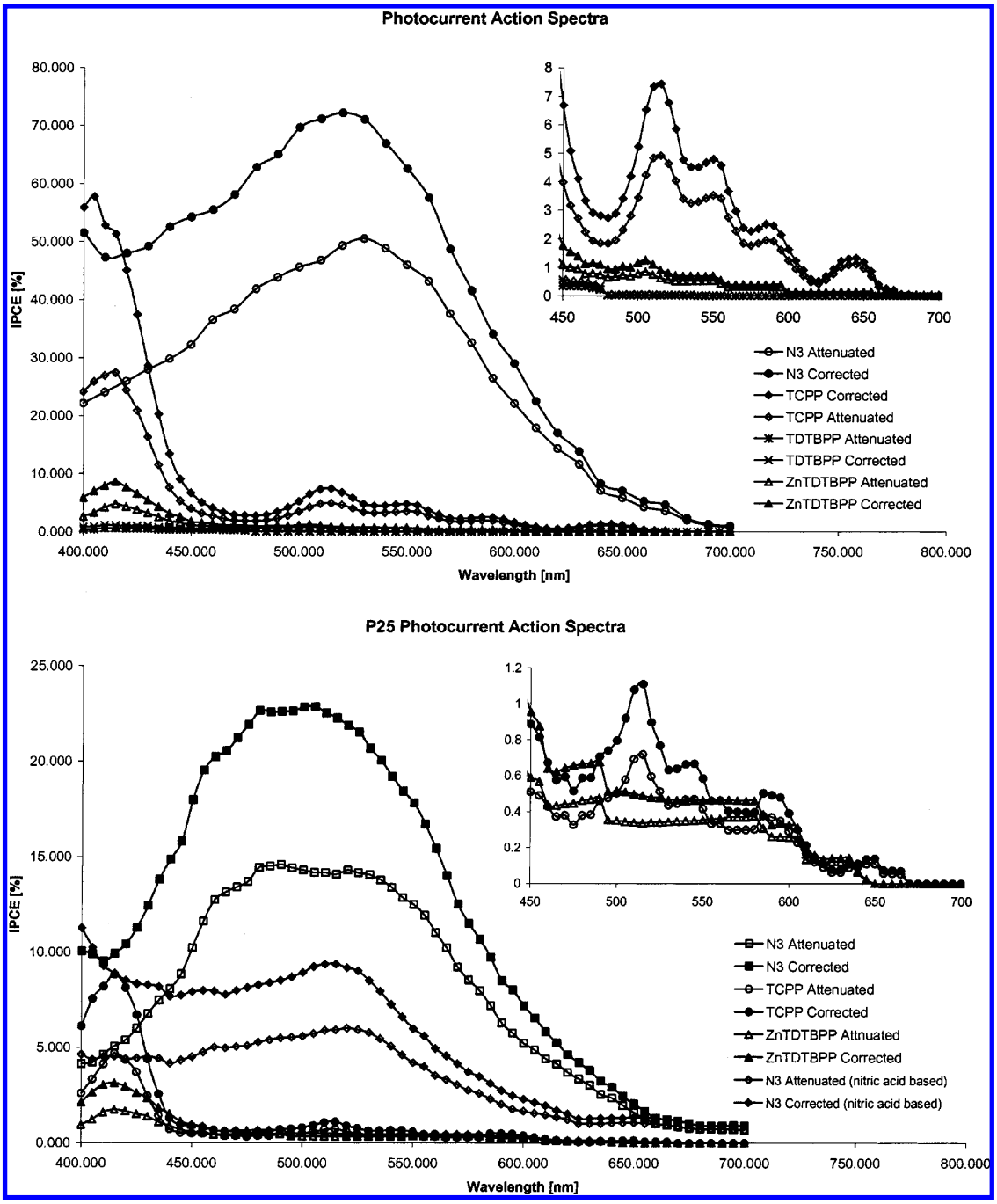

Figure 4. IPCE results of DSSCs constructed on (a) clear titania substrates and (b) P25 titania substrates. Both the corrected and attenuated results are shown to demonstrate the losses undergone due to the FTO glass used in this work.

attenuation due to the FTO was significant. This attenuation was taken into consideration and corrected for when calculations were performed on the various films. The errors associated with IPCE measurements were estimated to be as high as ±5%.

The best overall IPCE result observed was for the N3 system with efficiencies greater than 70% calculated over the 500−550-nm region as shown in Figure 4. From 400 (lower limit) to 630 nm, the N3-sensitized DSSCs displayed IPCE values in excess of 20%. Even at wavelengths beyond 630 nm electron injection was still occurring as evidenced by the tail in the spectral range (Figure 4). Comparison of these results to the absorption spectrum of N3 on titania in Figure 3 quickly revealed a direct correlation between the magnitude of the N3 extinction coefficient at various wavelengths and the IPCE curve at those wavelengths.

In the case of TCPP, the system IPCE values were as high as 60% in the range 400 to 450 nm in Figure 4. It was evident that upon comparison to the UV−vis spectrum of the dye on titania, electron injection in this region originated in the excitation of the Soret band. Q-band photoexcitation also contributed to the overall photocurrent at lower photon energies, with IPCE values ranging from 8% to 2%. A significant difference in the IPCE values between Soret and Q-band regions was not surprising considering the large differences in their respective extinction coefficients.

The tertbutyl-substituted porphyrin dye sensitizers, ZnDTBPP and TDTBPP, revealed far smaller IPCE values than both TCPP

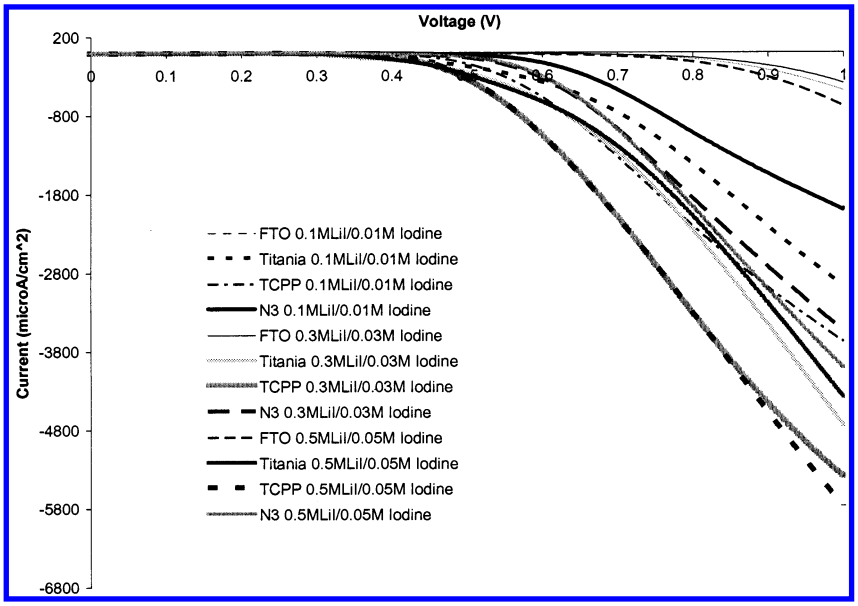

Figure 5. Dark current measurements comparing TCPP and N3 sensitized clear titania films, using different redox electrolyte concentrations.

and N3 based systems. Maximum efficiencies were 9% and 1%, respectively, both of which occurred in the Soret band region. No significant photocurrent associated with Q-band absorption was observed in either case.

Dark Current and Illuminated DSSC Current−Voltage Characteristic. The absorption of dye molecules onto porous titania electrodes is site specific and when combined with the effects of dye aggregation and desorption, many sites can remain vacant on the surface. This gives rise to the possibility of the adsorption of redox species to the surface. The reduction of redox species by photoinjected electrons may thus result in a negative overall current.[6] As such, a small overall exchange current is a criterion for negligible dark current at low potentials.[24] A Butler−Volmer activation model has been used to adequately describe the reduction of such adsorbed species.[25,20] In many ways dark current limitations have plagued photocurrent generation in DSSCs. Recent attempts to reduce the magnitude of dark currents have focused on passivating the electrode surface with functionalized redox-inactive pyridine derivatives such as 4-*tert*-butylpyridine. This has considerably increased cell performances by reducing the available surface sites for absorption of the active redox species (I_3^-).[26,27] In the present study, deoxycholic acid (DCA) was used to passivate the electrode surface after dye absorption. Our choice of DCA was guided by previous work, which showed it to be effective in this role with porphyrin-based DSSCs.[11] It has also been stated that DCA may prevent aggregation of the porphyrin dyes.[11]

Dark current measurements were performed on four different working electrode systems: (i) FTO glass, (ii) clear titania film, (iii) TCPP-sensitized titania film, and (iv) N3-sensitized titania film. In addition, three different electrolyte molarities (0.1 M LiI/0.01 M I_2, 0.3 M LiI/0.03 M I_2, 0.5 M LiI/0.0 5M I_2) were examined in each of the systems. All of the systems examined showed negligible dark current at low overpotentials as seen in Figure 5. In particular, system (i) demonstrated a very low dark current at overpotentials less than 0.6 V. However, systems (ii) to (iv) show rapidly increasing dark current more positive than 0.4 V (Figure 5). A close examination of the data reveals slight deviations between the various profiles. The variation of electrolyte molarity did not cause the dark current onset to change for the four systems studied; however, it did cause a large deviation in the dark current profile after the initial onset region. This effect was particularly noticeable for 0.1 M LiI/0.01 M I_2 electrolyte, but was also apparent for the 0.3 M LiI/0.03 M I_2 mixture at higher potentials.

Current−Voltage Results. The results obtained for current−voltage ($I-V$) scans for all systems when illuminated are shown in Figure 6. For an easier comparison of data, the DSSC efficiencies, η (%), short-circuit current densities, J_{SC}, open-circuit voltages, V_{OC}, and fill factors, FF, are summarized in Table 1. Correction for light attenuation by the FTO glass was considered in all efficiency calculations (24% power loss). As expected, comparison of the porphyrin-sensitized DSSC results to identically prepared N3-sensitized DSSCs revealed the N3-DSSCs to be superior ($\eta(\%) \approx 4$). Clear titania TCPP-sensitized DSSCs had much lower overall efficiencies ($\eta(\%) \approx 0.7$), overall. Although TCPP on clear films showed reasonable photocurrent results with $J_{SC} = 928(\pm 100)\ \mu A/cm^2$ and $V_{OC} = 344(\pm 40)$ mV (Table 1), N3 was the better sensitizer; $J_{SC} = 5345(\pm 300)\ \mu A/cm^2$ and $V_{OC} = 545(\pm 5)$ mV. The fill factors ranged between 0.49 and 0.61 for the porphyrin-based sensitizers.

Due to claims that porphyrin-based DSSCs experience a drastic increase in performance when cholanic acid derivatives were added to the sensitizing solution,[11] deoxycholic acid was used in this study for the TCPP systems. The results obtained with these cells performed far better than when no additive was employed. This has previously been attributed to a 2-fold action by these additives: (1) passivation of the titania surface reducing back electron transfer to the redox-active species and (2) prevention of surface aggregation by the porphyrin.[6]

Discussion

The theoretical aspects related to both observed photocurrents and dark currents have been formalized by Huang et al.[20] Briefly, the observed photocurrents (J_{ph}) can be described as being composed of two separate components across the semiconductor−electrolyte interface, the photoinjected current (J_{inj}) and the recombination current (J_r). By applying a modified Butler−Volmer equation, and realizing that $J_{inj} = J_r$ at V_{OC}, the open-circuit voltage dependence on the rate of back electron transfer (k_{et}), the concentration of I_3^- in the electrolyte (C_{ox}),

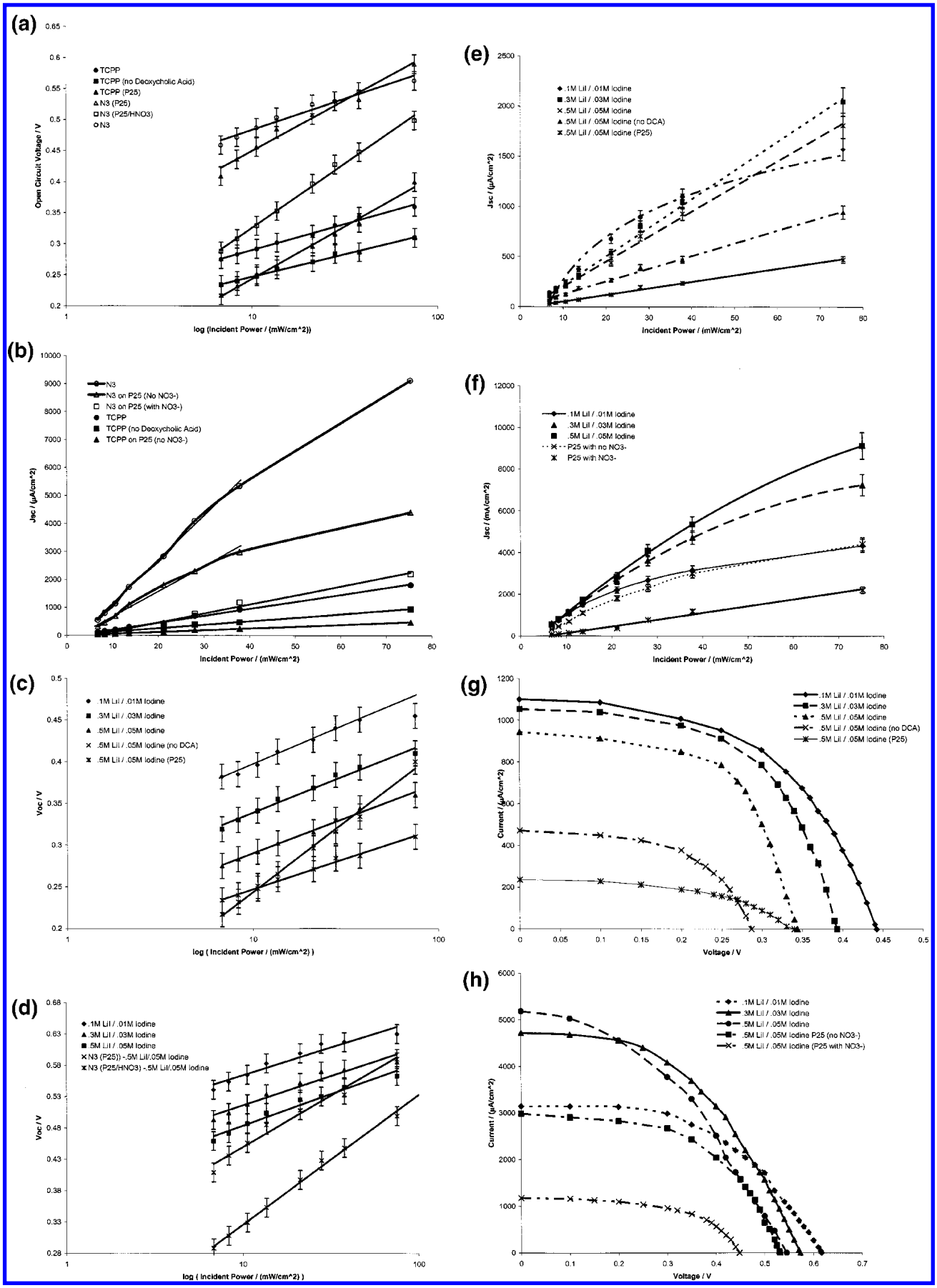

Figure 6. Complete set of results for cell $I-V$ characteristics. (a) V_{OC} vs ln I_0 and (b) J_{SC} vs I_0, for all cells, using 0.5 M LI/0.05 M I_2 electrolyte. Panels c and d show V_{OC} vs ln I_0 with varying electrolyte concentrations for TCPP and N3 sensitized cells, respectively. Panels e and f show J_{SC} vs I_0 with different electrolyte concentrations for the TCPP and N3 cells, respectively. Panels g and h show $I-V$ curves of TCPP and N3 cells at 37.85 mW/cm^2, respectively.

TABLE 1: Photocurrent Characteristics for the Sensitizer Systems Investigated at an Incident Power of 37.85 MW/cm^2 [a]

electrode	J_{sc} (μA/cm^2)	V_{oc} (mV)	fill factor	η (%)
TCPP	928	344	0.61	0.69
TCPP[b]	471	287	0.55	0.26
TCPP (P25)	235	334	0.5	0.15
TDTBPP	72	306	0.49	0.04
ZnTDTBPP	133	319	0.50	0.070

[a] The efficiencies shown here were corrected for 24% power loss due to attenuation caused by the FTO glass. [b] System did not contain DCA.

and the difference in the electron population in the semiconductor in the dark (n_0) and in the light (n) can be obtained (eq 2).

$$V_{OC} = \frac{k_B T}{qu\alpha}\left(\frac{AI_0}{k_{et} C_{ox}{}^{m} n_0{}^{u\alpha}}\right) \tag{2}$$

In eq 2, m is the order of reaction for the oxidized species, u is the order of reaction for the injected electrons, α is the electron-transfer coefficient, I_0 is the incident power, and A is the ratio of the absorbed flux to I_0. Algebraic manipulation of eq 2 allows $u\alpha$ to be expressed as a function of experimentally determinable values as shown by eq 3.

$$u\alpha = \frac{k_B T}{q}\left(\frac{dV_{OC}}{d \ln I_0}\right)^{-1} \tag{3}$$

The variation of I_0 with V_{OC} for each system displayed in Figure 6a shows a linear relationship between V_{OC} and ln I_0, a trend that is predicted by eq 3. The slope of the line in these systems can thus be directly related to the product $u\alpha$. Comparison of N3-sensitized and TCPP-sensitized DSSC data by using 0.5 M LiI/0.05 M I_2 electrolytes as shown in Figures 6 (0.0436 and 0.366, respectively) yields values of $u\alpha = 0.59$ and 0.7. This suggests that the mechanism for back electron transfer is similar. Interestingly the TCPP electrode prepared from a solution containing DCA also gave an identical $u\alpha$ value to a TCPP electrode prepared without DCA (Figure 6a). We interpret this result as an indication that the improvement in overall efficiency and IPCE that results from coadsorption of DCA with porphyrin sensitizers in DSSCs can mostly be attributed to the prevention of aggregation of the porphyrin dye by DCA.

In contrast to this, the mechanism of back electron transfer is clearly different for DSSCs constructed from P25. Once again these cells showed similar slopes for both N3- and TCPP-sensitized films with values of $u\alpha$ for N3 and TCPP being calculated to be 0.35 and 0.34, respectively. This strong dependence on the titania film cannot easily be explained. The capacitance of a particle has been found to be size dependent, which will in turn vary the electrical double layer at the semiconductor−electrolyte interface.[28] Such a phenomena will undoubtedly change the activation step on which the Butler−Volmer approach is based. Second, there is likely to be a difference in the surface reactivity caused by the presence of rutile in the P25. This too will affect the activation step and result in a change in the transfer coefficient, α. Interestingly, the slopes of ZnTDTBPP and TDTBPP were similar on clear titania films, but vastly different from those of N3 and TCPP. This highlights the strong correlation between chemical functionality and the electron-transfer coefficient, as neither of these dyes is able to form a covalent bond to the titania support.[6] By comparing the UV−vis absorption spectra results in Figure 3, it was clear that the dyes containing carboxylic acid functionality covered more sites on the titania surface. Slower recombination dynamics of porphyrin dyes with similarly bulky substituents to ZnTDTBPP and TDTBPP compared to TCPP has previously been shown to derive from a larger physical separation of the dye from the titania surface.[29] The exact nature of the differences is difficult to isolate, but may be related to the large difference in the availability of free sites for I_2 adsorption on the TiO_2 surface.[30]

Although the data plotted in Figure 6a are predominantly linear, the V_{OC} vs ln I_0 results do reveal a slight negative deviation when low concentrations of the I^-/I_2 redox couple are used at high incident light power conditions. It has been suggested that deviation from linearity occurs due to an increase in I_3^- concentration under high incident power. This lowers the electron concentration in TiO_2 and hence lowers V_{OC}.[20] Indeed, eq 2 predicts that such an increase (in [I_3^-]) will result in a decrease in V_{OC}. For the higher redox couple concentration electrolytes, 0.3 M LiI/0.03 M I_2 and 0.5 M LiI/0.05 M I_2 systems, a deviation of V_{OC} from linearity with incident power is most apparent in the N3-sensitized DSSCs. The much higher charge injection believed to occur with this sensitizer and the resulting increased [I_3^-] caused a more pronounced effect compared to porphyrin-sensitized DSSCs.

Previous studies have shown that I_{SC} increases linearly with incident light power.[13] The results obtained in this study accord with these findings for all systems showing photocurrent activity up to a light intensity of 40 mW/cm^2. A nonlinear photocurrent dependence on I_0 is discernible at higher incident light intensities in Figure 6b,c,d. This is most striking for the 0.1 M LiI/0.01 M I_2 system where photocurrents are likely to be diffusion limited. What is apparent from the data is the nonlinear tendency of N3 for higher I^-/I_2 concentrations. Diffusion limitations should not cause such behavior and as such the affect is believed to occur as a result of an increase in recombination rate at high photocurrents (at ca. >4 mA/cm^2).[31]

The Effect of Deoxycholic Acid. Consideration of the dark current results in Figure 5 indicated that the mechanism by which DCA enhances photocurrents in the porphyrin DSSCs is by aggregation prevention. We have also observed that TCPP DSSCs sensitized with DCA coadsorber present have increased open circuit voltages and photocurrents compared to cells prepared in the absence of DCA (Table 1). An alternative viewpoint previously put forward was that the effect of cholanic acids on porphyrin DSSCs (increased photovoltages and photocurrents) was due to a positive shift in the TiO_2 conduction band upon adsorption of cholanic acid.[11] It was suggested that the subsequent increase in thermodynamic driving force improved the electron injection efficiency. Although we cannot isolate antiaggregation effects from a shift in the TiO_2 conduction band here, we note that the dark current $I-V$ curves in Figure 5 for TCPP electrodes sensitized with and without DCA gave identical profiles. No change in the onset of the dark current was observed. Additionally DSSCs prepared by preadsorption of DCA are more effective than cells prepared by postadsorption. This would indicate that antiaggregation is the preponderant influence at work here, increasing photovoltages and photocurrents in porphyrin-containing DSSCs prepared with DCA as a coadsorber.

Comparison with Other Studies. The most recent study of $I-V$ characteristics of a TCPP-sensitized DSSC is that of Cherian and Wamser.[13] These authors were unable to measure absorption spectra below 500 nm due to intense light scattering from P25 films. In contrast, we were able to obtain complete

absorption spectra between 400 and 700 nm using semitransparent electrodes, from which we could ascertain distinct wavelength shifts of the Soret and Q-bands of TCPP. This is particularly noticeable as a red shift of the Q-bands (ca. 10-nm shift) upon absorption of TCPP on TiO_2. These shifts in band positions are considered to be an indication that TCPP effectively experiences a more polar environment when bound at the TiO_2 electrode compared to the ethanolic solution.[32] Cherian et al. also investigated adsorption, photoactivity, and the dependence of these properties upon surface complexation of the TCPP dye using XPS and resonance raman spectroscopy (RRS) for a DSSC constructed from a colloidal dispersion of Degussa P25. Their RRS results showed that when bare titania electrodes are sensitized by ethanolic solutions containing low concentrations of TCPP, distinct interactions between TCPP and TiO_2 may be discerned. On the other hand, at high concentrations porphyrin−porphyrin interactions dominate, presumably reducing the overall photovoltaic performance of the cell. Analysis of the Q-band region of the UV−vis absorption spectrum of Figure 3 indicates dye aggregation was minimal in solutions prepared from 0.1 mM TCPP/2 mM DCA. In IPCE measurements on electrodes prepared with ethanolic solutions of TCPP with and without deoxycholic acid as a coadsorber, the effectiveness of DCA for minimization of porphyrin−porphyrin interactions was noticeable (Table 1). Depending on the relative concentrations of the redox electrolyte used, we obtained similar values of V_{OC} (0.34−0.45 V compared to 0.46 V) and J_{SC} (928 μA/cm^2 compared to 170 μA/cm^2) to those of Cherian et al., with a similar fill factor (0.61 compared to 0.62).

The major difference between our IPCE results and the results obtained by others on P25-based titania DSSCs appears between 500 and 700 nm where the photocurrent is associated with the Q-bands. Our value at the Q-band maximum was 8% compared to Cherian et al.'s value of 45%. This discrepancy is puzzling, especially when a comparison between IPCE results between 400 and 500 nm where Soret-band absorption is expected to generate a photocurrent is carried out. In the Soret band region, both studies displayed a peak in the IPCE curve of 55−60%. We also compared our results for electrodes sensitized with N3 dye to IPCE curves in the literature and note that our photoaction spectrum matches these other studies.[6] We can thus be confident the result obtained for TCPP is not an artifact due to incorrect correction for FTO attenuation, or from deconvolution of the photoaction spectrum from the photodiode detector response curve. We do, however, note that the Soret band maximum in the absorption spectrum is approximately 10× larger than the highest Q-band peak.[14] The expectation is that the IPCE curve would reflect these changes in wavelength dependence of the extinction coefficient of TCPP-sensitized electrodes. This is indeed seen to be the case for our results shown in Figure 4.

Bignozzi et al. also obtained UV−vis absorption spectra and photoaction spectra for a number of substituted porphyrins including TCPP.[12] In this study DSSCs were constructed from transparent titania films produced by using a similar procedure to that described here.[33] Again the surface-bound TCPP Soret band maximum was typically 10× larger than the Q-band maximum and the photoaction spectum was observed to closely match the photoaction spectum. In calculating their IPCE results, however, reflective losses from their semitransparent titania electrode were neglected. The DSSCs were constructed by using a different electrolyte: 0.3 M TBAI/0.03 M I_2 in acetonitrile. Although the wavelength resolution of the resulting photoaction spectra was rather low, a maximum in the IPCE curve for TCPP of 10% could just be distinguished (coinciding with the Soret band absorption peak), the smaller Q-band peaks contributing less than 0.8%. We have taken into account factors such as reflective losses, but even the attenuated maximum in the IPCE curve in Figure 3 was 30%. Finally we note that others have demonstrated similar behavior for other porphyrin on P25-based DSSCs although low light irradiation was used (1 mW/cm^2) and IPCE maxima obtained (max ∼1%).[14]

Conclusion

As expected, N3 and TCPP dyes generated very high IPCE values compared to TDTBPP and ZnTDTBPP. The difference is ascribed to poor electronic coupling of the latter two sensitizers to the titania conduction band. Although the maximum obtainable open-circuit voltage is given by the difference between the titania Fermi level and the redox potential of the redox couple (ca. 0.97 V), dark current results show that obtaining this theoretical limit will be difficult. By considering the rate of reduction at the titania electrode it is evident that at higher photovoltages a rapid increase in the dark current will result. This causes the potential to drop significantly making the $I-V$ measurement diode-like in behavior. Using a better overall sensitizer like N3 (compared to TCPP) yielded a higher photovoltage and photocurrent.

Concentrating on TCPP-sensitized DSSCs, results on P25 films yielded much lower IPCE values than for DSSCs constructed from semitransparent titania electrodes (by a factor of 3−8 times over the AM1.5 wavelength range). The differences could be explained, in part, by the differences in the measured back electron transfer for DSSCs constructed from P25-based and 10 nm anatase TiO_2 colloid-based photoanodes. The photoaction spectrum closely matched the absorption spectrum for surface-bound TCPP, which we argue is more likely to occur than IPCE(λ) behavior observed in other studies.

Acknowledgment. We wish to acknowledge George Racz for excellent technical support and Geoff Will for many helpful discussions. We are grateful to Greg Wilson, John Bell, and Sustainable Technologies for their gift of N3 dye. M.J. and E.R.W. acknowledge support from SENRAC. J.J. and E.R.W. also acknowledge the IMRP, SPSC, and QUT (Strategic Collaborative Grant) for financial support in aid of this work.

References and Notes

(1) Hervás, M.; Navarro, J. A.; De La Rosa, M. A. *Acc. Chem. Res.* **2003**, *36*, 798−805. Herek, J. L.; Wohlleben, W.; Cogdell, R. J.; Zeidler, D.; Motzkus, M. *Nature* **2002**, *417*, 533−535.

(2) For an excellent description of the natural photosynthetic process see: Blankenship, R. E. *Molecular Mechanisms of Photosynthesis*; Blackwell Science Ltd.: Oxford, UK, 2002.

(3) Gregg, B. A.; Fox, M. A.; Bard, A. J. *J. Phys. Chem.* **1990**, *94*, 1586−1598.

(4) See: Gregg, B. A. *J. Phys. Chem. B* **2003**, *107*, 4688−4698. Gregg, B. A.; Hanna, M. C. *J. Appl. Phys.* **2003**, *93*, 3605−3614.

(5) Kalyanasundaram, K.; Vlachopoulos, N.; Krishnan, V.; Monnier, A.; Grätzel, M. *J. Phys. Chem.* **1987**, *91*, 2342−2347.

(6) Kalyanasundaram, K.; Grätzel, M. *Coord. Chem. Rev.* **1998**, *77*, 347−414.

(7) O'Regan, B.; Grätzel, M. *Nature* **1991**, *353*, 737−740.

(8) Hagfeldt, A.; Grätzel, M. *Acc. Chem. Res.* **2000**, *33*, 269−277.

(9) Ashbury, J. B.; Ellingson, R. J.; Ghosh, H. N.; Ferrere, S.; Nozik, A. J.; Lian, T. *J. Phys. Chem. B* **1999**, *103*, 3110−3119.

(10) Li, X.; Long, N. J.; Clifford, J. N.; Campbell, C. J.; Durrant, J. R. *New J. Chem.* **2002**, *26*, 1076−1080.

(11) Kay, A.; Grätzel, M. *J. Phys. Chem.* **1993**, *97*, 6272−6277. Kay, A.; Humphry-Baker, R.; Grätzel, M. *J. Phys. Chem.* **1994**, *98*, 952−959.

(12) Odobel, F.; Blart, E.; Lagrée, M.; Villieras, M.; Boujtita, H.; El Murr, N.; Caramori, S.; Bignozzi, C. A. *J. Mater. Chem.* **2003**, *13*, 502−510.

(13) Cherian, S.; Wamser, C. C. *J. Phys. Chem. B* **2000**, *104*, 3624−3629.

(14) Koehorst, R. B. M.; Boschloo, G. K.; Savenije, T. J.; Goossens, A.; Schaafsma, T. M. *J. Phys. Chem. B* **2000**, *104*, 2371−2377.
(15) Datta-Gupta, N.; Bardos, T. J. *J. Pharm. Sci.* **1968**, *57*, 300−304.
(16) Newman, M. S.; Lee, L. F. *J. Org. Chem*. **1972**, *37*, 4468−4479.
(17) Crossley, M. J.; King, L. G. *J. Chem. Soc., Chem. Commun.* **1984**, 920−922. Catalano, M. M.; Crossley, M. J.; Harding, M. M.; King, L. G. *J. Chem. Soc., Chem. Commun.* **1984**, 1535−1536.
(18) O'Regan, B.; Moser, J.; Anderson, M.; Grätzel, M. *J. Phys. Chem*. **1990**, *94*, 8720−8726.
(19) Ito, S.; Kitamura, T.; Wada, Y.; Yanagida, S. *Sol. Energy Mater. Sol. Cells* **2003**, *76*, 3−13.
(20) Huang, S. Y.; Schlichthörl, G.; Nozik, A. J.; Grätzel, M.; Frank, A. J. *J. Phys. Chem. B* **1997**, *101*, 2576−2582.
(21) Linsebigler, A. L.; Lu, G.; Yates, J. T. *Chem. Rev*. **1995**, *95*, 735−758.
(22) Wilgrome, L. R. *The Colours of Life*; Oxford University Press: New York, 1997.
(23) White, W. I. *The Porphyrins. Physical Chemistry Parts C and D*; Dolphin, D., Ed.; Academic Press: New York, 1978.
(24) Bard, A. J.; Faulkner, L. R. *Electrochemical Methods*; Wiley: New York, 1980.
(25) Ferber, J.; Luther, J. *J. Phys. Chem. B* **2001**, *105*, 4895−4903.
(26) Gregg, B. A.; Pichot, F.; Ferrere, S.; Fields, C. L. *J. Phys. Chem. B* **2001**, *105*, 1422−1429.
(27) Palomares, E.; Clifford, J. N.; Haque, S. A.; Lutz, T.; Durrant, J. R. *J. Am. Chem. Soc*. **2003**, *125*, 475−482.
(28) Schlichthörl, G.; Huang, S. Y.; Sprague, J.; Frank, A. J. *J. Phys. Chem. B* **1997**, *101*, 8141−8155.
(29) Clifford, J. N.; Yahioglu, G.; Milgrom, L. R.; Durrant, J. R. *Chem. Commun*. **2002**, 1260−1261.
(30) Fitzmaurice, D. J.; Eschle, M.; Frei, H.; Moser, J. *J. Phys. Chem*. **1993**, *97*, 3806−3812.
(31) Haque, S. A.; Tachibana, Y.; Willis, R. L.; Moser, J. E.; Grätzel, M.; Klug, D. R.; Durrant, J. R. *J. Phys. Chem. B* **2000**, *104*, 538−547.
(32) Gouterman, M. Optical Spectra and Electronic Structure of Porphyrins and Related Rings. In *The Porphyrins*; Dolphin, D., Ed.; Academic Press: New York, 1978; Vol. III, pp 1−165.
(33) Gillaizeau-Gauthier, I.; Odobel, F.; Alebbi, M.; Argazzi, R.; Costa, E.; Bignozzi, C. A.; Qu, P.; Meyer, G. J. *Inorg. Chem*. **2001**, *40*, 6073.
(34) Betsch, R. J.; Park, H. L.; White, W. B. *Mater. Res. Bull*. **1991**, *26*, 623−622.
(35) Cheng, H.; Ma, J.; Zhao, Z.; Qi, L. *Chem. Mater*. **1995**, *7*, 663−671.